Theoret. Appl. Mech., Vol.36, No.2, pp. 85–99, Belgrade 2009

Polynomial reconstruction of staggered unstructured vector fields

D. Vidović *

Abstract

Polynomial reconstruction of staggered unstructured vector fields has been considered. Coefficients of such polynomials are determined by the least squares method. Reduction in the rank of the least squares systems caused by the over-specification of the divergence may lead to difficulties. This has been investigated. The rank of these systems may be further reduced depending on the mesh geometry, or they may become ill conditioned. Guidelines for solving such linear systems have been presented.

Keywords: staggered unstructured grid, polynomial reconstruction, staggered vector field.

1 Introduction

For numerical approximation of the incompressible Navier-Stokes equations on Cartesian grids, the classical staggered Marker and Cell scheme of Harlow and Welch [3] is often the method of choice. The reasons are absence of spurious modes, local mass conservation, and the fact that artificial boundary conditions are not needed.

*Institute for the development of water resources "Jaroslav Černi", Belgrade, Serbia, E-mail: Dragan.Vidovic@jcerni.co.rs

Several generalizations of this scheme have been proposed for unstructured triangular meshes in [1, 2, 4, 5, 6, 7, 10, 11]. All these methods are first-order accurate in space on irregular meshes. Except [10, 11], the schemes described are restricted to incompressible flows. Second order accurate schemes for incompressible and compressible flows have been presented in [8, 9].

In staggered grids the pressure and the velocity are stored in different points. The usual choice is to store the pressure in the cells, as well as the other scalars, and to associate normal velocity components with the faces. This is illustrated in Fig. 1.

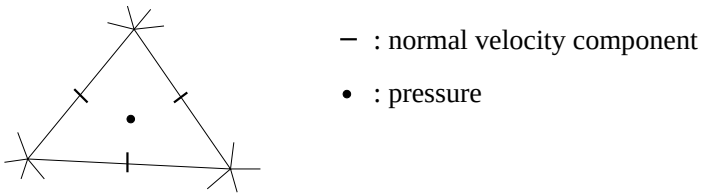

Figure 1: Staggered positioning of the variables in an unstructured grid.

Since the velocity vector is not known in any point, the preprocessing and the postprocessing stages are more complicated than in the collocated case. Additional difficulties that arise on unstructured grids may be the reason why the staggered unstructured schemes are not widely accepted.

The main problem in the design of unstructured staggered schemes is the reconstruction of the velocity vector in certain points of interest. Some techniques to achieve this on a triangular grid in two dimensions and difficulties that arise are presented in this paper. The three dimmensional case is similar.

2 Staggered vector field

In a staggered grid the velocity field $\mathbf{u}$ is represented by its averaged normal components

$$u_e = \frac{1}{l_e} \int_e (\mathbf{u} \cdot \mathbf{N}_e) dl, \tag{1}$$

where $\mathbf{N}_e$ is one of the two possible unit normal vectors to face e, and l_e is the length of this face. Such choice allows an exact discretization of the velocity divergence:

$$\int_\Omega (\nabla \cdot \mathbf{u})\, d\Omega = \oint_{\partial\Omega} (\mathbf{u} \cdot \mathbf{n})\, d\Gamma = \sum_{e=1}^{3} u_e \bar{l}_e, \tag{2}$$

where $\bar{l}_e = (\mathbf{N}_e \cdot \mathbf{n}_e)\, l_e$, n_e is the outward normal to face e, and Ω is a triangle.

3 Piecewise constant reconstruction

The scheme developed in [8, 9] uses the following reconstruction to compute a vector component in a cell:

$$\mathbf{N} \cdot \mathbf{u} \approx \xi_i u_i + \xi_j u_j, \tag{3}$$

where i and j are two faces of this cell, $\mathbf{N}$ is an arbitrary unit vector, and ξ_i and ξ_j are chosen such that

$$\mathbf{N} = \xi_i \mathbf{N}_i + \xi_j \mathbf{N}_j. \tag{4}$$

This reconstruction is exact for piecewise constant vector fields only. Other expressions of the same order of accuracy are found in the literature.

4 Piecewise linear reconstruction

In order to obtain higher order schemes, the velocity vector field needs to be reconstructed from staggered data with sufficient accuracy. To approximate $\mathbf{u}$ in the vicinity of point with coordinate vector $\mathbf{r}_0$, we postulate a piecewise linear approximation of the following form:

$$\mathbf{u}(\mathbf{r}) \approx \mathbf{P}(\mathbf{r}) = \mathbf{a} + \mathbf{b}x + \mathbf{c}y, \tag{5}$$

where $\mathbf{r} = [xy]^T$ is the position vector of a point where u is to be reconstructed, relative to point r_0. Point r_0 may be a face center, a cell

centroid, or a vertex. We want to determine **a**, **b** and **c** such that the face average of $\mathbf{N}_e \cdot \mathbf{P}(\mathbf{r})$ matches the normal components u_e for face e belonging to a certain set (that will be called the *reconstruction stencil*) as closely as possible in the least squares sense. Fig. 2 shows possible reconstruction stencils. This leads to the following linear system:

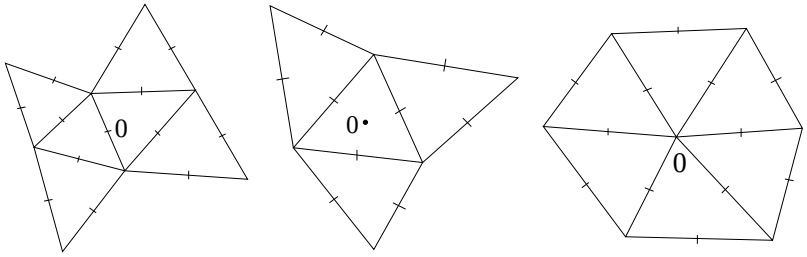

Figure 2: Examples of reconstruction stencils for face-based (left), cell-based (middle) and vertex-based (right) linear reconstruction.

$$\mathbf{N}_e \cdot \mathbf{P}(\mathbf{r}_e) = u_e, \qquad \text{for each face } e \text{ in the reconstruction stencil,} \quad (6)$$

where $\mathbf{r}_e$ is the coordinate of the center of face e relative to r_0. This system can be written as

$$Mc = u, \quad (7)$$

where

$$M = \begin{bmatrix} N_{x,1} & N_{y,1} & N_{x,1}x_1 & N_{x,1}y_1 & N_{y,1}x_1 & N_{y,1}y_1 \\ \vdots & \vdots & \vdots & \vdots & \vdots & \vdots \\ N_{x,k} & N_{y,k} & N_{x,k}x_k & N_{x,k}y_k & N_{y,k}x_k & N_{y,k}y_k \end{bmatrix}, \quad (8)$$

$$c = \begin{bmatrix} a_1 & a_2 & b_1 & b_2 & c_1 & c_2 \end{bmatrix}^T, \quad u = \begin{bmatrix} u_1 & \dots & u_k \end{bmatrix}^T, \quad (9)$$

and k is the number of faces in the reconstruction stencil.

If the tangential velocity component u_e^t is prescribed as a boundary condition in some of the boundary faces belonging to the reconstruction stencil, equation

$$\mathbf{T}_e \cdot \mathbf{P}(\mathbf{r}_e) = u_e^t \quad (10)$$

is added to system (6) where $\mathbf{T}_e = (-N_{y,e}, N_{x,e})$ and $u_e^t = \mathbf{T}_e \cdot \mathbf{u}_e$. This can be done for all faces in the reconstruction stencil where the tangential velocity is prescribed, or only for the faces closer to the center of the reconstruction stencil.

In order to determine the least squares solution for c it is necessary that $\text{rank}(M) = 6$. If $\text{rank}(M) < 6$, the stencil needs to be enlarged, or the degree of P must be lowered. On general unstructured grids it is difficult to specify a priori reconstruction stencils such that $\text{rank}(M) = 6$. However, we can say the following: if a reconstruction stencil contains one triangle Ω, the rank of M will be lowered by one by adding constraint

$$\nabla \cdot \mathbf{u} = b_1 + c_2 = \frac{1}{|\Omega|} \oint_{\partial\Omega} \mathbf{n} \cdot \mathbf{P}(\mathbf{r}) d\Gamma = \frac{1}{|\Omega|} \sum_{e=1}^{3} \mathbf{N}_e \cdot \mathbf{P}(\mathbf{r}_e) \bar{l}_e \qquad (11)$$

(see (2) and (6)). Each triangle in the reconstruction stencil adds such a constraint, and therefore

$$\text{rank}(M) \leq k - \tilde{k} + 1, \qquad (12)$$

where $\tilde{k}$ is the number of triangles in the reconstruction stencil. Hence, for the stencil in Fig. 3 we have $\text{rank}(M) \leq 5$, so this stencil is too small, and additional faces must be added.

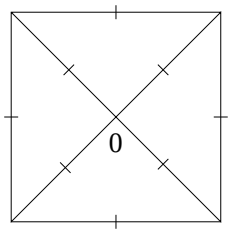

Figure 3: Insufficient reconstruction stencil for vertex-based linear reconstruction.

An additional rank reduction may occur in special situations. Fig 4 shows an enlarged vertex-based reconstruction stencil for a boundary vertex 0. Face centers 1, 2 and 3 are collinear, so there exist coefficients

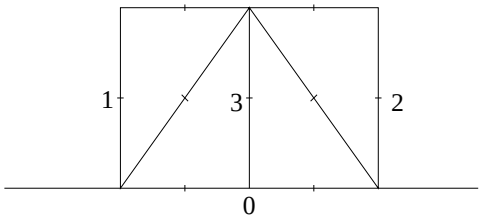

Figure 4: Reconstruction stencil at a boundary.

α and β such that $\mathbf{r}_3 = \alpha\mathbf{r}_1 + \beta\mathbf{r}_2$ and $\alpha + \beta = 1$. In the case presented in Fig. 4, $\alpha = \frac{1}{2}$ and $\beta = \frac{1}{2}$. These faces are also parallel, and we shall suppose that $\mathbf{N}_1 = \mathbf{N}_2 = \mathbf{N}_3$. By substituting this in the left hand side of the equation (6) for face 3 we obtain

$$\mathbf{N}_3 \cdot \mathbf{P}(\mathbf{r}_3) = \mathbf{N}_3 \cdot \mathbf{P}(\alpha\mathbf{r}_1 + \beta\mathbf{r}_2) = \alpha\mathbf{N}_1\mathbf{P}(\mathbf{r}_1) + \beta\mathbf{N}_2\mathbf{P}(\mathbf{r}_2). \tag{13}$$

The equation for face 3 is linearly dependent on the equations for faces 1 and 2, and $\mathrm{rank}(M) \leq k - \tilde{k} + 1 - 1 < 6$.

If the grid is unstructured, stencils close to the stencil of Fig. 4 frequently appear at boundaries, resulting in ill-conditioned linear systems. In order to detect such situations, singular value decomposition (SVD) is used to find the pseudo-inverse of M. The stencil is enlarged if some singular value is less than some threshold. Because the matrices involved are small, SVD takes only a small part of total computing time.

In order to match the normal velocities in the faces closer to the center more closely than those in the outer part of the reconstruction stencil, we use weight 1 for the equations related to the central faces, and 10^{-2} for all the others. Central faces are the faces meeting in the central vertex in the case of the vertex-based reconstruction, faces of the central triangle in the case of the cell-based reconstruction, or the faces of the two central triangles in the case of the face-based reconstruction. This gives practically absolute priority to the nearest neighbors, but still keeps the singular values of the reconstruction matrix relatively large. Numerical experiments have shown that in this matrix two groups of singular values can be distinguished: those proportional to the larger weight, and those proportional to the smaller weight. For this reason using too small weights

can have negative effect on the accuracy. Using ratio 1/1000 gives almost the same results. Results are not very sensitive to this parameter.

Still, matrix $M^T M$ emerging from (6) when the least squares or the SVD method is used becomes very ill-conditioned as the mesh is refined. This problem is also present in the 1d case. Requirement that a one-dimensional polynomial of degree $n-1$ has specified values in points $x_1, \ldots, x_n$ results in Vandermonde matrix. Determinant of this matrix is $\prod_{i>j}(x_i - x_j)$. As points x_i get closer to each other, the matrix approaches a singular one. Our situation is similar. In order to avoid growing ill-conditioning, we scale $\mathbf{r}_i$ by some typical length h, for example the length of the central face, the square root of the area of the central cell, or the average length of the faces meeting in the central vertex. Hence, in (5)–(7) instead of $\mathbf{r}$ and $\mathbf{P}$ we use

$$\tilde{\mathbf{r}} = \begin{bmatrix} \tilde{x} & \tilde{y} \end{bmatrix}^T = \frac{\mathbf{r}}{h}, \quad \tilde{\mathbf{P}}(\tilde{\mathbf{r}}) = \mathbf{P}(\mathbf{r}) = \mathbf{a} + \tilde{\mathbf{b}}\tilde{x} + \tilde{\mathbf{c}}\tilde{y}, \quad \tilde{\mathbf{b}} = h\mathbf{b}, \quad \tilde{\mathbf{c}} = h\mathbf{c}. \tag{14}$$

We solve for the scaled coefficients $\mathbf{a}$, $\tilde{\mathbf{b}}$ and $\tilde{\mathbf{c}}$, which are used to calculate $\mathbf{b}$ and $\mathbf{c}$.

The coefficients of the linear polynomial are obtained in the form

$$[a_1, \ldots c_2]^T = M^+ \cdot [u_1, \ldots u_k]^T, \tag{15}$$

where M^+ is the pseudo-inverse of matrix M. In codes that solve partial differential equations, systems like (7) have to be solved many times with different right hand sides. However, matrix M^+ depends only on the grid and on the weights. Therefore it can be calculated in advance. This implies that a $6 \times k$ matrix must be stored for each vertex, cell, or face.

4.1 Divergence-free linear reconstruction

Since $b_1 + c_2 = \nabla \cdot \mathbf{P}$ in (5), we can require that

$$b_1 + c_2 = d = \nabla \cdot \mathbf{u} \tag{16}$$

exactly, where the divergence is computed as in (2):

$$d = \frac{1}{|\Omega|} \int_\Omega (\nabla \cdot \mathbf{u}) d\Omega = \frac{1}{|\Omega|} \sum_{e=1}^{k_1} u_e \bar{l}_e. \tag{17}$$

Let $b_1 = d/2 + b$, $c_2 = d/2 - b$, and

$$\overline{\mathbf{P}}(\mathbf{r}) = \mathbf{a} + \begin{bmatrix} b & c_1 \\ b_2 & -b \end{bmatrix} \mathbf{r}. \tag{18}$$

Note that $\nabla \cdot \overline{\mathbf{P}} = 0$; therefore $\overline{\mathbf{P}}$ will be called the *divergence-free part* of $\mathbf{P}$. The reconstruction polynomial with specified divergence d can be represented in the following way:

$$\mathbf{P}(\mathbf{r}) = \overline{\mathbf{P}}(\mathbf{r}) + \frac{d}{2}\mathbf{r}. \tag{19}$$

The number of free parameters has dropped from six to five.

Each face e in the reconstruction stencil contributes the following equation:

$$\mathbf{N}_e \cdot \overline{\mathbf{P}}(\mathbf{r}_e) = u_e - \frac{1}{2}(\mathbf{N}_e \cdot \mathbf{r})d. \tag{20}$$

The least squares solution is given by

$$\begin{bmatrix} a_1 \\ a_2 \\ b \\ c_1 \\ b_2 \end{bmatrix} = M^+ \cdot \left(\begin{bmatrix} u_1 \\ \vdots \\ u_k \end{bmatrix} - \frac{1}{2} \begin{bmatrix} N_{x,1}x_1 + N_{y,1}y_1 \\ \vdots \\ N_{x,k}x_k + N_{y,k}y_k \end{bmatrix} d \right), \tag{21}$$

where M^+ is the pseudo-inverse of the matrix M of system (20). We substitute (17) in (21) in order to obtain

$$\begin{bmatrix} a_1 \\ a_2 \\ b \\ c_1 \\ b_2 \end{bmatrix} = M^+ \cdot \left(\begin{bmatrix} u_1 \\ \vdots \\ u_k \end{bmatrix} - \frac{1}{2\,|\Omega|} \begin{bmatrix} N_{x,1}x_1 + N_{y,1}y_1 \\ \vdots \\ N_{x,k}x_k + N_{y,k}y_k \end{bmatrix} \begin{bmatrix} \bar{l}_1 & \dots & \bar{l}_{k_1} \end{bmatrix} \cdot \begin{bmatrix} u_1 \\ \vdots \\ u_{k_1} \end{bmatrix} \right). \tag{22}$$

In this way faces used to specify the divergence d enter the reconstruction stencil.

If at least five faces meet in a vertex, they impose enough conditions to determine the solenoidal part of a vertex-based linear polynomial (see Fig. 5 on the left and in the middle). However, if fewer than five faces meet in some vertex, the stencil is enlarged as in Fig. 5 on the right (or the order of interpolation must be lowered.

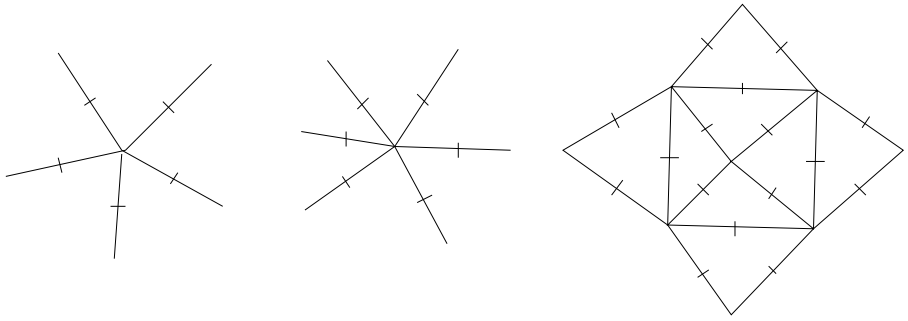

Figure 5: Reconstruction stencils for the divergence-free vertex-based linear reconstruction.

5 Piecewise quadratic reconstruction

We postulate

$$\mathbf{u}(\mathbf{r}) \approx \mathbf{P}(\mathbf{r}) = \mathbf{a} + \mathbf{b}x + \mathbf{c}y + \mathbf{d}x^2 + \mathbf{e}xy + \mathbf{f}y^2. \tag{23}$$

We have 12 free parameters. The stencils shown in Fig. 2 do not contain enough information to determine these parameters, so we must enlarge them. An example of an appropriate cell-based stencil is shown in Fig. 6.

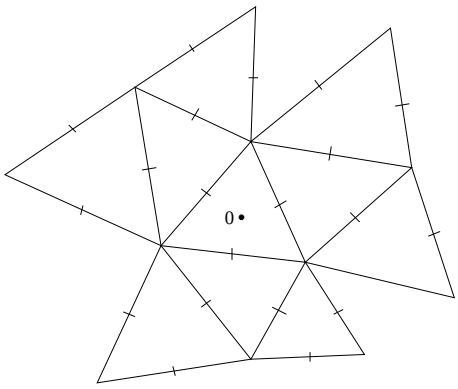

Figure 6: Reconstruction stencil for cell-based quadratic reconstruction.

Our primary velocity variables are not the normal velocities in the face centers but their averages along these faces. For this reason, instead of $\mathbf{N}_e \cdot \mathbf{P} = u_e$ we need to satisfy

$$\frac{1}{l_e}\int_e \mathbf{N}_e \cdot \mathbf{P} dl = u_e \tag{24}$$

The average of a linear polynomial along a face is equal to the value of the polynomial in the center of that face, and this is why condition (6) was good enough in the linear case. In order to evaluate (24) we need the averages of x^2, xy and y^2 over the faces. Face e is parameterized as $x = x_e + tl_{x,e}, y = y_e + tl_{y,e}$, $t \in [-1/2, 1/2]$, where $(l_{x,e}, l_{y,e})$ is the vector of face e and x_e and y_e are the coordinates of the face center. Then

$$\begin{aligned} \frac{1}{l_e}\int_e x^2 dl = \frac{1}{l_e}\int_{-\frac{1}{2}}^{\frac{1}{2}} (x_e + tl_{x,e})^2 l_e dt = x_e^2 + \frac{l_{x,e}^2}{12}, \\ \frac{1}{l_e}\int_e xy dl = x_e y_e + \frac{l_{x,e} l_{y,e}}{12}, \\ \frac{1}{l_e}\int_e y^2 dl = y_e^2 + \frac{l_{y,e}^2}{12}. \end{aligned} \tag{25}$$

Each face e in the reconstruction stencil contributes with the following equation:

$$\begin{aligned} N_{x,e}a_1 + N_{y,e}a_2 + N_{x,e}x_e b_1 + N_{y,e}x_e b_2 + N_{x,e}y_e c_1 + N_{y,e}y_e c_2 + \\ + N_{x,e}\left(x_e^2 + \frac{l_{x,e}^2}{12}\right) d_1 + N_{y,e}\left(x_e^2 + \frac{l_{x,e}^2}{12}\right) d_2 + \\ + N_{x,e}\left(x_e y_e + \frac{l_{x,e} l_{y,e}}{12}\right) e_1 + N_{y,e}\left(x_e y_e + \frac{l_{x,e} l_{y,e}}{12}\right) e_2 + \\ + N_{x,e}\left(y_e^2 + \frac{l_{y,e}^2}{12}\right) f_1 + N_{y,e}\left(y_e^2 + \frac{l_{y,e}^2}{12}\right) f_2 = u_e. \end{aligned} \tag{26}$$

If the tangential vector component is given in this face, the appropriate equation is obtained by replacing $\mathbf{N}_e$ by $\mathbf{T}_e$ and u_e by u_e^t .

As in the linear case, we combat rounding errors by scaling by h, and actually use $\tilde{\mathbf{r}}$ instead of $\mathbf{r}$ in (23). Later we transform the coefficients of

this scaled polynomial into the coefficients of the original one by dividing the coefficients with linear terms by h and the coefficients with quadratic terms by h^2.

5.1 Divergence-free quadratic reconstruction

The divergence of a quadratic polynomial is a linear function

$$\nabla \cdot \mathbf{P}(\mathbf{r}) = b_1 + c_2 + (2d_1 + e_2)x + (e_1 + 2f_2)y = \alpha + \beta x + \gamma y. \quad (27)$$

It is required that $\nabla \cdot \mathbf{P}(\mathbf{r})$ matches the divergence of the reconstructed vector in at least three triangles as closely as possible in the least squares sense. For example, if a cell-based quadratic polynomial is being calculated, then the divergence is calculated from the central and the three surrounding triangles in Fig. 6. For each of these triangles the following equation needs to be satisfied as closely as possible:

$$\int_\Omega (\alpha + \beta x + \gamma y) d\Omega = \sum_e u_e \bar{l}_e, \quad (28)$$

where the summation runs over the faces of triangle Ω. From these conditions parameters α, β and γ are calculated. By substituting (27) in (23) one obtains

$$\begin{aligned} P_x(\mathbf{r}) = &\quad a_1 + (\alpha/2 + b)x + c_1 y + d_1 x^2 + (\gamma - 2f_2)xy + f_1 y^2 \\ P_y(\mathbf{r}) = &\quad a_2 + b_2 x + (\alpha/2 - b)y + d_2 x^2 + (\beta - 2d_1)xy + f_2 y^2 \end{aligned} \quad (29)$$

When the system (24) is formed, terms containing α, β and γ are moved to the right hand side, and the rest is calculated in analogy with the linear case.

6 Piecewise cubic reconstruction

We consider cubic polynomials:

$$\mathbf{P}(\mathbf{r}) = \mathbf{a} + \mathbf{b}x + \mathbf{c}y + \mathbf{d}x^2 + \mathbf{e}xy + \mathbf{f}y^2 + \mathbf{g}x^3 + \mathbf{h}x^2 y + \mathbf{i}xy^2 + \mathbf{j}x^3. \quad (30)$$

Here we have 20 free parameters. The stencil is obtained by choosing faces closest to the stencil center until the rank is 20 and all singular values are sufficiently large. Typical stencil contains around 30 faces.

In the similar manner as before, we shall need the following integrals:

$$\begin{aligned} I_{x^3} &= \frac{1}{l_e}\int_e x^3 dl = x_e^3 + x_e\frac{l_{x,e}^2}{4}, \\ I_{x^2y} &= \frac{1}{l_e}\int_e x^2 y dl = x_e^2 y_e + \frac{l_{x,e}}{12}(l_{x,e}y_e + 2l_{y,e}x_e), \\ I_{xy^2} &= \frac{1}{l_e}\int_e xy^2 dl = x_e y_e^2 + \frac{l_{y,e}}{12}(2l_{x,e}y_e + l_{y,e}x_e), \\ I_{y^3} &= \frac{1}{l_e}\int_e y^3 dl = y_e^3 + y_e\frac{l_{y,e}^2}{4}. \end{aligned} \tag{31}$$

For each face e in the reconstruction stencil the following equation needs to be satisfied as closely as possible in the least squares sense:

$$\begin{aligned} &N_{x,e}a_1 + N_{y,e}a_2 + N_{x,e}x_e b_1 + N_{y,e}x_e b_2 + N_{x,e}y_e c_1 + N_{y,e}y_e c_2 + \\ &+N_{x,e}I_{xx}d_1 + N_{y,e}I_{xx}d_2 + N_{x,e}I_{xy}e_1 + N_{y,e}I_{xy}e_2 + N_{x,e}I_{yy}f_1 + N_{y,e}I_{yy}f_2 + \\ &+N_{x,e}I_{x^3}g_1 + N_{y,e}I_{x^3}g_2 + N_{x,e}I_{x^2y}h_1 + N_{y,e}I_{x^2y}h_2 + \\ &+N_{x,e}I_{xy^2}i_1 + N_{y,e}I_{xy^2}i_2 + N_{x,e}I_{y^3}j_1 + N_{y,e}I_{y^3}j_2 = u_e, \end{aligned} \tag{32}$$

where

$$I_{xx} = x_e^2 + \frac{l_{x,e}^2}{12}, \qquad I_{xy} = x_e y_e + \frac{l_{x,e}l_{y,e}}{12}, \qquad I_{yy} = y_e^2 + \frac{l_{y,e}^2}{12}. \tag{33}$$

It is possible to make divergence-free cubic reconstruction in an analogous way to the linear and the quadratic case.

7 Conclusion

Several methods for reconstruction of staggered vector fields have been presented, together with some difficulties that arise on unstructured grids. Vertex-based divergence-free linear reconstruction has several advantages. It leads to a smaller reconstruction stencil, and it requires roughly half

the memory of the non-divergence-free linear reconstruction. It does not need weights, thresholds or SVD whenever at least five faces meet in a vertex or if the tangential velocity is prescribed in a sufficient number of faces meeting in the central vertex.

Quadratic and cubic reconstruction require large reconstruction stencils. It is difficult to determine in advance which faces need to enter the reconstruction stencil, and the computer code must implement some sort of a trial and error approach. It has been demonstrated in [8, 9] that vertex-based divergence-free linear reconstruction is accurate enough to obtain second-order accuracy when solving Navier-Stokes equations.

References

[1] C.A. Hall, J.C. Cavendish, and W.H. Frey. The dual variable method for solving fluid flow difference equations on Delaunay triangulations. *Computers and Fluids*, 20:145–164, 1991.

[2] C.A. Hall, T.A. Porsching, and P. Hu. Covolume-dual variable method for thermally expandable flow on unstructured triangular grids. *Int. J. Comp. Fluid Dyn.*, 2:111–139, 1994.

[3] F.H. Harlow and J.E. Welch. Numerical calculation of time-dependent viscous incompressible flow of fluid with a free surface. *The Physics of Fluids*, 8:2182–2189, 1965.

[4] R.A. Nicolaides. The covolume approach to computing incompressible flows. In M.D. Gunzburger and R.A. Nicolaides, editors, *Incompressible Computational Fluid Dynamics*, pages 295–333, Cambridge, UK, 1993. Cambridge University Press.

[5] R.A. Nicolaides, T.A. Porsching, and C.A. Hall. Covolume methods in computational fluid dynamics. In M. Hafez and K. Oshima, editors, *Computational Fluid Dynamics Review 1995*, pages 279–299, Chichester, 1995. Wiley.

[6] B. Perot. Conservation properties of unstructured staggered mesh schemes. *J. Comp. Phys.*, 159:58–89, 2000.

[7] S. Rida, F. McKenty, F.L. Meng, and M. Reggio. A staggered control volume scheme for unstructured triangular grids. *Int. J. Num. Meth. in Fluids*, 25:697–717, 1997.

[8] D. Vidović, A. Segal, and P. Wesseling. A superlinearly convergent finite volume method for the incompressible Navier-Stokes equations on staggered unstructured grids. *Journal of Computational Physics*, 198:159–177, 2004.

[9] D. Vidović, A. Segal, and P. Wesseling. A superlinearly convergent Mach uniform finite volume method for the Euler equations on staggered unstructured grids. *Journal of Computational Physics*, 2005. Accepted with revisions.

[10] I. Wenneker, A. Segal, and P. Wesseling. A Mach-uniform unstructured staggered grid method. *International Journal for Numerical Methods in Fluids*, 40:1209–1235, 2002.

[11] I. Wenneker, A. Segal, and P. Wesseling. Conservation properties of a new unstructured staggered scheme. *Computers and Fluids*, 32:139–147, 2003.

Submitted on January 2008, revised on

Polinomijalna rekonstrukcija razdeljenih nestruktuiranih vektorskih polja

Razmatra se polinomialna rekonstrukcija razdeljenih nestruktuiranih vektorskih polja. Koeficijenti takvih polinoma se odreduju metodom najmanjih kvadrata. Smanjenje ranga sistema najmanjih kvadrata uzrokovano preodredenjem divergencije može da dovede do teškoća. Ovo je ispitano. Rank ovih sistema može biti još više umanjen u zavisnosti od geometrije mreže, ili oni mogu postati slabo uslovljeni. Predstavljene su vodilje za rešavanje takvih linearnih sistema.

doi:10.2298/TAM0902085V Math.Subj.Class.: 41A10, 76M12